Published in final edited form as:
Magn Reson Imaging. 2015 January ; 33(1): 43–50. doi:10.1016/j.mri.2014.10.001.

Effect of Hepatocyte-Specific Gadolinium-Based Contrast Agents on Hepatic Fat-Fraction and R2*

Diego Hernando, Ph.D.[1], **Shane A. Wells, M.D.**[1,5], **Karl K. Vigen, Ph.D.**[1], and **Scott B. Reeder, M.D., Ph.D.**[1,2,3,4]

[1] Department of Radiology, University of Wisconsin – Madison, Madison, WI, United States

[2] Department of Medical Physics, University of Wisconsin – Madison, Madison, WI, United States

[3] Department of Biomedical Engineering, University of Wisconsin – Madison, Madison, WI, United States

[4] Department of Medicine, University of Wisconsin – Madison, Madison, WI, United States

[5] Department of Radiology, University of Virginia, Charlottesville, VA

Abstract

The purpose of this work was to investigate the effect of a hepatocyte-specific gadolinium based contrast agent (GBCA) on quantitative hepatic fat-fraction (FF) and R2* measurements. Fifty patients were imaged at 1.5T, using chemical-shift encoded water-fat MRI with low (5°) and high (15°) flip angles (FA), both before and after administration of a hepatocyte-specific GBCA (gadoxetic acid). Low and high FA, pre- and post-contrast FF and R2* values were measured for each subject. Available serum laboratory studies related to liver disease were also recorded. Linear regression and Bland-Altman analysis were performed to compare measurements. Hepatic FF was unaffected by GBCA at low FA (slope=1.02±0.02,p=0.32). FF was overestimated at high FA pre-contrast (slope=1.33±0.03,$p<10^{-10}$), but underestimated post-contrast (slope=0.81±0.02,$p<10^{-10}$). Hepatic R2* was unaffected by FA (mean difference±95% CI pre-contrast:2.2±4.9s^{-1}, post-contrast:2.8±3.6s^{-1}), but increased post-contrast in patients with total bilirubin <2.5 mg/dL ($\Delta R2^*$=13.4±12.7s^{-1}). Regression analysis of serum values demonstrated a correlation of post-contrast change in R2* with total bilirubin ($p<0.01$) and model for end-stage liver disease (MELD) score ($p\approx0.01$). In conclusion, GBCA has no effect on hepatic FF at low FA due to a lack of T1-weighting, potentially allowing flexibility for FF imaging with hepatobiliary imaging protocols. Hepatic R2* increased significantly after GBCA administration, particularly in the biliary tree. Therefore, R2* maps should be obtained prior to contrast administration.

Correspondence: Diego Hernando Ph.D. L1115 WIMR 1111 Highland Ave Madison, WI 53705 dhernando@wisc.edu.

Keywords

gadoxetic acid; fat-water imaging; fat quantification; iron quantification; R2*; fat-fraction

Introduction

In recent years, several MRI-based techniques have been introduced for accurate, reproducible quantification of fat-fraction and R2* (=1/T2*) as biomarkers of liver fat content and hepatic iron overload, respectively. These techniques are based on multi-echo chemical shift encoded water-fat separation techniques that rely on signal estimation models for estimation of fat-fraction and R2* (1-16). As part of the technical refinement of these methods, several confounding factors have been identified and addressed to ensure accurate quantification of fat and iron in the liver. For fat quantification, these include the effects of T1 related bias (9,17,18), R2* correction (3,5,9,19), spectral complexity of fat (5,11,20), noise related bias (17), and more recently, phase-shifts induced by eddy currents (4,21,22). Upon correction for all relevant confounding factors, fat quantification techniques produce maps of proton density fat-fraction (PDFF), which is a fundamental biomarker of tissue triglyceride concentration (23,24).

For quantification of R2*, it is now recognized that fat is a confounding factor of R2* measurements. To avoid this confounder, it is necessary to perform simultaneous estimation of fat and water signals in addition to R2* mapping (25-27). Extensive validation of these techniques, particularly for fat quantification has been performed in phantoms (11,16,28,29), animal models (12), and more recently in large human studies comparing MRI techniques to MR spectroscopy (6-8,13). Several manufacturers have recently introduced commercial products or investigational prototypes of confounder-corrected fat-fraction and R2* mapping techniques, and widespread availability of these methods is expected in the near future.

In addition, there has been a recent increase in the use of hepatocyte-specific gadolinium-based contrast agents (GBCA), particularly with gadoxetic acid (Eovist/Primovist, Bayer Pharmaceutical, Wayne, NJ), which was approved by the FDA in 2008. Gadoxetic acid is increasingly used for liver specific imaging, as it has approximately 50% uptake into hepatocytes with subsequent excretion into bile ducts. It has been used extensively for improving the sensitivity of detection and characterization of liver lesions (30-37) as well as functional biliary imaging in diseases such as primary sclerosing cholangitis (38,39). After administration of gadoxetic acid, a substantial amount of gadolinium is taken up into hepatocytes and dramatic alterations in MR relaxivity, particularly T1 and T2*, takes place. It is well known that differences in T1 between water and fat can introduce bias in quantification of fat-fraction. Prior to contrast administration, water signal has considerably longer T1 than fat (e.g., typical T1 for liver water and fat signals are 586 ms and 343 ms, respectively, at 1.5T) (17). Therefore, it is expected that the presence of GBCA may impact quantification of liver fat-fraction and R2*.

Yokoo et al. have previously investigated the effects of extracellular fluid (ECF) GBCA's on the ability to quantify liver fat (18). Yokoo et al. found that the use of a high flip angle after the administration of an ECF GBCA resulted in normalization of the fat-fraction without any

T1 related bias. The authors hypothesized that the relative T1 between water and fat in the liver was normalized, i.e. approximately equal, in the presence of this GBCA. However, Yokoo et al. only considered in- and opposed-phase (IOP) fat-water imaging, instead of confounder-corrected chemical shift-encoded fat quantification (6,13,40). Further, the authors did not study the effect of hepatocyte specific contrast agent on liver fat quantification. To date, only preliminary accounts of this effect have been reported (41,42). Therefore, the purpose of this work was to investigate the impact of a hepatocyte-specific GBCA, gadoxetic acid, on the quantification of hepatic FF and R2* using a previously validated, confounder-corrected chemical shift encoded quantitative MRI technique (6,13,40). In addition, FF and R2* measurements before and after contrast administration were compared with serum analysis values, including serum measures of liver dysfunction and severity of chronic liver disease.

Materials and Methods

Patient Population

After obtaining institutional review board approval and informed consent, 50 patients (25 males, 25 females, average age of 50.3±17.1 years, range = 18 - 84) were scanned prospectively. The patients were scanned with the following indications or diagnoses: 1: incidental liver lesion seen on CT or ultrasound (13 patients), 2: known or suspected metastatic disease (10 patients), 3: known or suspected biliary abnormality (eg. gallstones, choledochal cyst) (10 patients), 4: primary sclerosing cholangitis (PSC) (7 patients), 5: liver transplant (4 patients), 6: elevated liver enzymes not otherwise specified (4 patients), 7: cholangiocarcinoma (2 patients), 8: primary biliary cirrhosis (1 patient). Note that one of the patients had a known diagnosis of both PSC and cholangiocarcinoma and is listed in both categories above. Imaging was performed at 1.5 T (Signa HDxt and Optima MR 450w, GE Healthcare, Waukesha, WI), using an 8 or 12 channel phased array cardiac or body coil used for conventional liver imaging.

Clinical data

The patients' clinical records were retrospectively reviewed. If available, body mass index (BMI), and blood analysis results within 3 months before or after imaging were recorded. Blood analysis measurements that were recorded included total bilirubin, aspartate aminotransferase (AST), alanine aminotransferase (ALT), gamma-glutamyl transpeptidase (GGT), alkaline phosphatases, creatinine, international normalized ratio (INR), and albumin. The model for end-stage liver disease (MELD) score was calculated for patients not taking coumadin using the recorded values of serum bilirubin, serum creatinine and INR (43).

Pulse Sequences

All MR imaging for this study was performed using an investigational version of a confounder corrected, chemical shift encoded water-fat separation method (6,13,40) that has been previously validated for quantification of PDFF. This is a quantitative imaging technique that provides both PDFF as well as an R2* map obtained as part of the R2*-corrected PDFF (5,6). Specific imaging parameters for this spoiled gradient echo (SPGR) acquisition included: 3D axial slab, $TR/TE_1/\Delta TE$ = 13.5/1.2/2.0 ms, echo train length = 6,

matrix = (224-256) × 160 × 32, 36 × 32 cm field of view, 8mm slices, readout bandwidth between ±83 kHz and ±125 kHz. A data-driven, Autocalibrating Reconstruction for Cartesian imaging (ARC) parallel imaging technique was used to reduce scan time to approximately 21 seconds with an effective acceleration of 3.2 (44). Overall true spatial resolution was (1.4-1.6) × 2.2 × 8 mm^3.

Prior to the administration of contrast, two acquisitions were obtained, one with a low flip angle (5°), previously shown to minimize T1 related bias in PDFF measurement, and the other with a high flip angle (15°), used to intentionally create T1 bias in the FF measurement. Therefore, high flip angle imaging provided an apparent fat-fraction, which was not expected equal to PDFF. The same two acquisitions were repeated approximately 20 minutes after the intravenous bolus administration of 0.05 mmol/kg of gadoxetic acid, injected at a rate of 2.0 ml/s followed by a 25 ml saline chase. The time between the injection of contrast and the post contrast chemical shift encoded acquisition was recorded.

In summary, four chemical shift-encoded acquisitions were performed on each subject: pre-contrast with small flip angle, pre-contrast with large flip angle, post-contrast with small flip angle and post-contrast with large flip angle. Reconstruction of fat-fraction maps and R2* maps for each of the four acquisitions was performed with an on-line reconstruction algorithm that provides DICOM fat-fraction and R2* maps. The on-line reconstruction algorithm incorporates R2* correction, spectral modeling of fat, magnitude discrimination technique to avoid noise related bias, and eddy current correction (4,5,17). The pre-contrast, low flip angle fat-fraction maps, which have been validated in previous studies (6,8,13), are used as reference for PDFF measurement.

Imaging Data Analysis

Fat-fraction and R2* values were measured from pre- and post- contrast fat-fraction and R2* maps at both low and high flip angles using regions of interest (ROI) from all nine Couinaud segments of the liver. ROIs were initially placed on the pre-contrast, low flip angle PDFF maps, avoiding large vessels or bile ducts, and then copied to the corresponding locations on the remaining pre-contrast and post-contrast fat-fraction and R2* maps. ROI's were carefully adjusting for respiratory variation and obvious artifacts. The fat-fraction and R2* values were averaged across segments for each subject, for each acquisition.

Statistical Analysis

Fat-fraction values measured with low flip angle and high flip angle were compared using linear regression and Bland-Altman analysis. In addition, fat-fraction values obtained before and after the administration of contrast were also compared using linear regression and Bland-Altman analysis. Hepatic R2* values before and after contrast were compared using linear regression, and R2* values obtained with high and low flip angle, both before and after contrast, were compared using linear regression and Bland-Altman analysis to detect any differences between these measurements.

Additionally, these imaging measurements were compared with the patients' available clinical data. Specifically, FF (pre-contrast, low FA), R2* (pre-contrast, high FA) and ΔR2*=R2* (post-contrast, high FA)- R2* (pre-contrast, high FA) were each compared to the

BMI and blood analysis measurements described above. Further, FF, R2* and ΔR2* were compared pairwise with each other. Comparisons were performed using linear regression analysis on the logarithms of the measurements (excluding negative measurements) to create a uniform spread of data in the regression. A total of 36 linear regressions were performed. The p-value for the null hypothesis that the slope=0 was calculated in each case. To account for the large number of regressions (i.e. to avoid excessive type-I errors), the sequential Holm-Šidàk procedure was applied to the p-values (45). This is a simple procedure where the individual p-values are sequentially updated (increased) to reflect the fact that a family of tests (rather than a single test) is being performed. After this procedure was applied, p-values smaller than 0.05 were considered statistically significant.

Finally, the measured increase in R2* post-contrast (ΔR2*) was compared using linear correlation to the time after contrast administration (in minutes) after which the post-contrast R2* and FF maps were acquired. The purpose of this comparison was to assess the temporal behavior of the effects of GBCA on R2* and FF quantification.

Results

The average time after the administration of gadoxetic acid for which post contrast PDFF and R2* maps were obtained was 19.9±5.8 minutes (range = 5-37 minutes).

Figure 1 illustrates an example of fat-fraction maps obtained in a 43-year-old man with hepatic steatosis with a corresponding hepatic fat-fraction of 19.1% (measured with the low flip-angle pre-contrast sequence). As seen in this figure, prior to the administration of the contrast, the apparent fat-fraction increases to 24.4% when a high flip angle is used. This apparent increase in fat-fraction is the result of T1 bias; the T1 of fat signal in the liver is known to be shorter than the T1 of water signal (46). There is no substantial difference in hepatic fat-fraction at a low flip angle following contrast administration compared to the reference standard pre-contrast, low flip angle fat fraction (18.7% compared to 19.1%). The similarity of these measurements illustrates the ability of low flip-angle imaging to provide T1-independent measures of PDFF. However, the fat-fraction observed following the administration of contrast at a high flip angle was lower than the reference standard pre-contrast, low flip angle fat fraction (16.8% compared to 19.1%). After the administration of gadoxetic acid, a decrease in the apparent fat fraction at the high flip angle was observed. This reversal of T1 bias in the presence of intracellular contrast agent implies the T1 of water signal becomes *shorter* than the T1 of fat signal due to the effect of intracellular accumulation of gadoxetic acid within hepatocytes.

Figure 2 summarizes the fat quantification results from all subjects confirming this overall behavior. Using low flip angles, hepatic fat fraction was not affected in the presence of intracellular gadolinium (ie: T1-independent PDFF). Using high flip angles prior to contrast administration, the apparent hepatic fat fraction is overestimated because the T1 of fat in the liver is shorter than the T1 of water.

Figure 3 shows an example of a 44-year-old woman with focal fat in segment IVa, as depicted in both in-phase and opposed-phase post-contrast images as well as in fat-fraction

maps. Bias in high flip-angle focal fat quantification for this patient was in good agreement with that observed in the patients with diffuse fat deposition.

Figure 4 summarizes the R2* measurement results from all subjects confirming a clear increase in hepatic R2* following the administration of gadoxetic acid. As expected, there was no substantial difference in hepatic R2* between low and high flip angles. Averaged across all subjects, for both low and high flip angles, the apparent hepatic R2* increased by 13.6 s^{-1}, from a pre-contrast average of 31.6 s^{-1} to a post-contrast average of 45.2 s^{-1}. Although there was a trend for $\Delta R2^*>0$, this was not significant when considering all patients (95% CI at low flip angle: $12.4\pm13.7s^{-1}$, high flip angle: $13.0\pm15.9s^{-1}$). As evident on the pre-contrast R2* measurements, only one of the subjects had elevated liver iron (liver R2* above 60 s^{-1}) (47); however, there are several additional subjects with apparent R2* above 60 s^{-1} on R2* maps generated following contrast administration. This could potentially lead to false positive diagnoses of hepatic iron overload, if hepatic R2* was measured after the administration of gadoxetic acid.

Figure 5 demonstrates an example of R2* map obtained before and after administration of gadoxetic acid in a 26-year-old woman with two hepatic masses with imaging findings consistent with focal nodular hyperplasia (FNH). The post-contrast R2* maps clearly depict the FNH (including the central scar), as well as the biliary tree and areas of subcapsular fibrosis. Note the higher R2* (relative to the liver parenchyma) in the periphery of the FNH, indicating higher gadolinium accumulation in the lesion compared to the liver. This is consistent with the appearance of the hyperintense rim of these lesions on the 20-minute delayed post-contrast T1 weighted images.

Figure 6 demonstrates T1-weighted fat-saturated images and the corresponding R2* maps before and after administration of gadoxetic acid in a 36-year-old man with cirrhosis related to primary sclerosing cholangitis, and documented hepatic dysfunction. There is relatively little accumulation of gadolinium observed on the delayed post-contrast images, acquired 20 min after contrast injection. Notice that there is little change in the apparent hepatic R2* on the post-contrast R2* maps. This example suggests that accumulation of gadoxetic acid in the liver correlates with an increase in apparent hepatic R2* following contrast administration and reflects the poor underlying hepatic function of this patient.

Upon retrospective review of the patients' clinical data, BMI was available from 43 patients, bilirubin from 39 patients, AST from 40 patients, ALT from 41 patients, GGT from 14 patients, alkaline phosphatase from 37 patients, creatinine from 40 patients, INR from 27 patients, albumin from 31 patients, platelets from 37 patients, and MELD scores from 24 patients. After performing the Holm procedure to account for the large number of linear regressions performed, only two pairwise comparisons resulted in slopes significantly different from zero: total bilirubin vs $\Delta R2^*$ and MELD vs $\Delta R2^*$ (see Figure 7): $\Delta R2^*$ had a negative correlation with both total bilirubin and MELD scores. Bland-Altman analysis of R2* pre- and post-contrast revealed a significant increase in R2* among patients with total bilirubin < 2.5 mg/dL (mean±95% CI: low flip angle: $12.7\pm10.9s^{-1}$, high flip angle: $13.4\pm12.7s^{-1}$), but no increase among patients with total bilirubin ≥ 2.5mg/dL (mean±95% CI at low flip angle: $1.0\pm5.1s^{-1}$, high flip angle: $-0.9\pm10.5s^{-1}$).

Additionally, seven pairwise comparisons had slopes significantly different from zero before, but not after, the Holm procedure: AST vs ΔR2*, BMI vs PDFF, MELD vs PDFF, ALT vs ΔR2*, alkaline phosphatases vs ΔR2*, alkaline phosphatases vs PDFF, and bilirubin vs PDFF. These comparisons might require a larger number of subjects in order to achieve statistical significance. Details are not included for the sake of scope and brevity.

Finally, a comparison between the delay time after contrast (in minutes) and ΔR2* (in s^{-1}) is shown in Figure 8. Note that including very short (<10 min) and very long (>34 min) times results in a significant increase in ΔR2* with time after contrast, but excluding these extreme values results in little correlation between ΔR2* and time after contrast.

Discussion

In this work we have investigated the effects of gadoxetic acid on quantitative MRI biomarkers of hepatic steatosis (PDFF) and iron overload (R2*). Specifically the effects of gadoxetic acid on T1 related bias for measuring PDFF and R2* maps were prospectively investigated and measured. This work demonstrated that if the effects of T1 bias are mitigated through the use of a proton density weighting (achieved by use of a low flip angle), there is minimal effect of gadoxetic acid on quantification of hepatic fat-fraction. Therefore, this study demonstrates that measurements of fat-fraction after the administration of gadoxetic acid are valid, so long as a low flip angle is used to avoid the effects of T1 related bias. The low flip angle results are consistent with those obtained by Yokoo et al using a different contrast agent (extracellular fluid GBCA).

This work also demonstrated “reversed” T1 bias with fat quantification after the administration of gadoxetic acid when a high flip angle was used. This result differs from the prior work by Yokoo et al, where the presence of extracellular GBCA resulted in similar fat quantification using either low or high flip angles. In this study, we anticipated some change in the apparent fat-fraction due to T1 weighting; however, given the significant differences between gadoxetic acid (a hepatocyte-based GBCA) and an extracellular fluid GBCA, the exact nature of this change was unknown *a priori*. Further, the technique used in this study (confounder-corrected PDFF measurement) is significantly different from the technique used by Yokoo et al (in-phase and opposed-phase imaging). The results from this study clearly demonstrate a decrease in the apparent fat-fraction using a higher flip angle after the administration of gadoxetic acid, and indicate that high flip angle imaging should not be used for hepatic fat quantification either before or after administration of gadoxetic acid. These results also demonstrate that the T1 of water must be shorter than the T1 of fat after the uptake of gadoxetic acid into hepatocytes. This differential signal change in hepatic T1 in the presence of intracellular gadolinium may provide some interesting new insights into the pharmacokinetics and cellular compartmentalization of gadoxetic acid. Gadoxetic acid accumulates in the cytoplasm of hepatocytes via transport by the organic anion transported protein (48). The observed fat signal arises from triglycerides that have accumulated in intracellular vacuoles, also located within the cytoplasm. The reversal of T1 bias that was observed indicates that hepatic accumulation of gadoxetic acid preferentially shortens the T1 of free water to a much greater extent than the T1 of triglycerides (if this is affected at all). In recent pre- and post-contrast T1 measurements of liver water and fat

performed using spectroscopy at 3T (49), a similar water and fat T1 was found post-contrast, whereas our results suggest a shorter T1 of water compared to fat post-contrast. This discrepancy may be due to differences in the dose of gadoxetic acid employed. Further experiments examining the separate T1 of water and fat components would be required to understand the detailed mechanism of the change in T1 bias observed with high flip angles after gadoxetic acid administration.

In patients with normal hepatic synthetic function according to the total bilirubin measured from blood analysis, this work also demonstrates a significant increase in hepatic R2* after the administration of gadoxetic acid. If hepatic R2* were to be measured following the administration of gadoxetic acid, the apparent hepatic R2* would be elevated, potentially resulting in a false positive diagnosis of elevated liver iron concentration. Thus, hepatic R2* should be quantified prior to the administration of gadoxetic acid if attempting to measure the underlying R2* of the hepatic parenchyma.

Note that the effect of gadoxetic acid on R2* does not affect hepatic fat-fraction measurements because confounder-corrected fat-fraction estimation is R2*-corrected. However, fat-quantification techniques that do not account for R2* decay may be confounded by the presence of gadoxetic acid, even if low flip angles are used to avoid T1 related bias.

Importantly, no correlation was observed between PDFF and pre-contrast liver R2* measurements. Note that R2* measurements are corrected for the spectral complexity of the fat signal. This is in good agreement with recent results from a biopsy correlation study by Kühn et al (25). Interestingly, in several of the patients with severe chronic disease (e.g.. cirrhosis, primary sclerosing cholangitis), there was a relative lack of hepatic accumulation of gadoxetic acid. This was demonstrated in both the qualitative T1 weighted acquisitions used as part of the diagnostic examination, and by the lack of change in the hepatic R2* values observed following contrast administration. This raises the speculation that changes in hepatic R2* before and after the administration of gadoxetic acid may serve as potential quantitative biomarker for hepatic function. Numerous authors have attempted to use changes in signal intensity on T1 weighted images in order to measure such liver function (46-50). To the best of our knowledge, no attempts had been made previously to measure hepatocyte function using gadoxetic acid coupled with quantitative R2* maps. In our results, a lack of increase of R2* after contrast administration was correlated with elevated values of both total bilirubin and MELD scores, which are measures of liver function and severity of chronic liver disease. Future work will be needed to further characterize whether changes in R2* with gadoxetic acid administration could be used to quantify hepatic function.

Regarding the impact of gadoxetic acid on the quantification of R2*, a limitation of this study is that only one of the patients had elevated liver R2* pre-contrast. Therefore, it is difficult to determine the impact of gadoxetic acid on R2* in a patient with iron overload. In several patients, the hepatic R2* increased above the threshold commonly used to diagnose iron overload (47), following the administration of contrast. Further work is needed to determine the overall impact of gadoxetic acid on hepatic R2* in patients with iron overload and the ability to stage moderate or severe iron overload in the presence of this contrast.

Although a reference standard, such as MR spectroscopy or tissue sampling, was not used to validate the low flip angle hepatic fat-fraction measurements obtained in this study, Meisamy (6) and Hines, et al. (13) recently validated this technique in patients using MR spectroscopy as reference standard, and Idilman et al validated this method compared to biopsy (40). These studies demonstrated, with excellent correlation and agreement, that this imaging protocol and reconstructions are statistically equivalent to quantitative MR spectroscopy techniques. Therefore, PDFF maps obtained with a low flip angle prior to contrast should form a valid reference standard for quantifying hepatic fat-fraction.

An additional consideration is that a dose of 0.05 mmol/kg of gadoxetic acid was used. The recommended (package insert) dose of gadoxetic acid is 0.025 mmol/kg, based on the minimum effective dose for delayed hepatobiliary phase imaging. However, recent data suggests that 0.025 mmol/kg of gadoxetic acid yields inadequate dynamic phase enhancement compared to 0.1 mmol/kg of gadobenate dimeglumine (MultiHance, Bracco Diagnostics, Inc), and that the use of 0.05 mmol/kg improves diagnostic accuracy (39,50,51). In addition, Frydrychowicz, et al. recently demonstrated that 0.1 mmol/kg of gadobenate dimeglumine provided superior dynamic phase enhancement compared to 0.05 mmol/kg of gadoxetic acid (52). Despite the fact that this is twice the recommended dose of gadoxetic acid, it is still half the gadolinium dose of other conventional contrast agents, and therefore, from a safety perspective, results in reduced exposure to patients who may be at risk of nephrogenic systemic fibrosis (NSF). For these reasons, a dose of 0.05 mmol/kg gadoxetic acid is the standard of care at our institution. The use of a lower dose of gadoxetic acid would likely result in similar trends but with smaller changes in R2* and high flip angle apparent fat-fraction between pre- and post-contrast quantification. Specifically, the ability of low flip-angle imaging to accurately measure hepatic fat-fraction would likely be maintained in the presence of a lower dose of gadoxetic acid.

In summary, this work has demonstrated that fat-fraction measurements are valid after the administration of gadoxetic acid provided T1-weighting is avoided through the use of low flip angles or other techniques that compensate for potential T1 related bias. Quantification of R2*, however, is impacted in the presence of gadoxetic acid and post-contrast R2* values may not accurately reflect the underlying iron concentration in the liver. Understanding the impact of hepatocyte-specific GBCA on fat-fraction and R2* measurements may be helpful for improving protocol workflow and the flexibility of abdominal MRI. For example, if only fat-fraction imaging is desired, it may be more time efficient to perform quantitative fat-fraction imaging after the administration of gadolinium prior to a 20 minute delayed hepatobiliary phase image, improving the overall work flow of the acquisition. We do not recommend this approach for quantification of R2*. Further, this work demonstrated a decrease in hepatic fat fraction in the presence of gadoxetic acid and T1-weighting (i.e. when using high flip angles). These observations, as well as the observation that post-contrast R2* did not change in patients with cirrhosis, may provide new opportunities to explore the pharmacokinetics of gadoxetic acid in the normal liver and in patients with diffuse liver disease.

Acknowledgements

We acknowledge the support of the NIH (RC1 EB010384, R01 DK083380, R01 DK088925, and R01 DK096169), and the Wisconsin Alumni Research Foundation (WARF) Accelerator Program. We also thank GE Healthcare for their support.

References

1. Reeder, SB.; Hines, CDG.; Yu, H.; McKenzie, CA.; Brittain, JH. On the definition of fat-fraction for in vivo fat quantification with magnetic resonance imaging. International Society for Magnetic Resonance in Medicine Honolulu; HI: 2009. p. 211
2. Reeder SB, Robson PM, Yu H, Shimakawa A, Hines CD, McKenzie CA, Brittain JH. Quantification of hepatic steatosis with MRI: the effects of accurate fat spectral modeling. J Magn Reson Imaging. 2009; 29:1332–1339. [PubMed: 19472390]
3. Yu H, McKenzie CA, Shimakawa A, Vu AT, Brau AC, Beatty PJ, Pineda AR, Brittain JH, Reeder SB. Multiecho reconstruction for simultaneous water-fat decomposition and T2* estimation. J Magn Reson Imaging. 2007; 26:1153–1161. [PubMed: 17896369]
4. Yu H, Shimakawa A, Hines CD, McKenzie CA, Hamilton G, Sirlin CB, Brittain JH, Reeder SB. Combination of complex-based and magnitude-based multiecho water-fat separation for accurate quantification of fat-fraction. Magn Reson Med. 2011; 66:199–206. [PubMed: 21695724]
5. Yu H, Shimakawa A, McKenzie CA, Brodsky E, Brittain JH, Reeder SB. Multiecho water-fat separation and simultaneous R2* estimation with multifrequency fat spectrum modeling. Magn Reson Med. 2008; 60:1122–1134. [PubMed: 18956464]
6. Meisamy S, Hines CD, Hamilton G, Sirlin CB, McKenzie CA, Yu H, Brittain JH, Reeder SB. Quantification of hepatic steatosis with T1-independent, T2-corrected MR imaging with spectral modeling of fat: blinded comparison with MR spectroscopy. Radiology. 2011; 258:767–775. [PubMed: 21248233]
7. Yokoo T, Bydder M, Hamilton G, Middleton MS, Gamst AC, Wolfson T, Hassanein T, Patton HM, Lavine JE, Schwimmer JB, Sirlin CB. Nonalcoholic fatty liver disease: diagnostic and fat-grading accuracy of low-flip-angle multiecho gradient-recalled-echo MR imaging at 1.5 T. Radiology. 2009; 251:67–76. [PubMed: 19221054]
8. Yokoo T, Shiehmorteza M, Hamilton G, Wolfson T, Schroeder ME, Middleton MS, Bydder M, Gamst AC, Kono Y, Kuo A, Patton HM, Horgan S, Lavine JE, Schwimmer JB, Sirlin CB. Estimation of hepatic proton-density fat fraction by using MR imaging at 3.0 T. Radiology. 2011; 258:749–759. [PubMed: 21212366]
9. Bydder M, Yokoo T, Hamilton G, Middleton MS, Chavez AD, Schwimmer JB, Lavine JE, Sirlin CB. Relaxation effects in the quantification of fat using gradient echo imaging. Magn Reson Imaging. 2008; 26:347–359. [PubMed: 18093781]
10. Bydder M, Yokoo T, Yu H, Carl M, Reeder SB, Sirlin CB. Constraining the initial phase in water-fat separation. Magn Reson Imaging. 2011; 29:216–221. [PubMed: 21159457]
11. Hernando D, Liang ZP, Kellman P. Chemical shift-based water/fat separation: a comparison of signal models. Magn Reson Med. 2010; 64:811–822. [PubMed: 20593375]
12. Hines CD, Agni R, Roen C, Rowland I, Hernando D, Bultman E, Horng D, Yu H, Shimakawa A, Brittain JH, Reeder SB. Validation of MRI biomarkers of hepatic steatosis in the presence of iron overload in the ob/ob mouse. J Magn Reson Imaging. 2012; 35:844–851. [PubMed: 22127834]
13. Hines CD, Frydrychowicz A, Hamilton G, Tudorascu DL, Vigen KK, Yu H, McKenzie CA, Sirlin CB, Brittain JH, Reeder SB. T(1) independent, T(2) (*) corrected chemical shift based fat-water separation with multi-peak fat spectral modeling is an accurate and precise measure of hepatic steatosis. J Magn Reson Imaging. 2011; 33:873–881. [PubMed: 21448952]
14. Eggers, H.; Perkins, TG.; Hussain, SM. Influence of spectral model and signal decay on hepatic fat fraction measurements at 3T with dual-echo Dixon imaging.. Proceedings of the 19th Annual Meeting of ISMRM; Montreal, Canada. 2011; p. 573
15. Hu HH, Perkins TG, Chia JM, Gilsanz V. Characterization of human brown adipose tissue by chemical-shift water-fat MRI. AJR Am J Roentgenol. 2013; 200:177–183. [PubMed: 23255760]

16. Lee SS, Lee Y, Kim N, Kim SW, Byun JH, Park SH, Lee MG, Ha HK. Hepatic fat quantification using chemical shift MR imaging and MR spectroscopy in the presence of hepatic iron deposition: validation in phantoms and in patients with chronic liver disease. J Magn Reson Imaging. 2011; 33:1390–1398. [PubMed: 21591008]
17. Liu CY, McKenzie CA, Yu H, Brittain JH, Reeder SB. Fat quantification with IDEAL gradient echo imaging: correction of bias from T(1) and noise. Magn Reson Med. 2007; 58:354–364. [PubMed: 17654578]
18. Yokoo T, Collins JM, Hanna RF, Bydder M, Middleton MS, Sirlin CB. Effects of intravenous gadolinium administration and flip angle on the assessment of liver fat signal fraction with opposed-phase and in-phase imaging. J Magn Reson Imaging. 2008; 28:246–251. [PubMed: 18581393]
19. O'Regan DP, Callaghan MF, Wylezinska-Arridge M, Fitzpatrick J, Naoumova RP, Hajnal JV, Schmitz SA. Liver fat content and T2*: simultaneous measurement by using breath-hold multiecho MR imaging at 3.0 T--feasibility. Radiology. 2008; 247:550–557. [PubMed: 18349314]
20. Hamilton G, Yokoo T, Bydder M, Cruite I, Schroeder ME, Sirlin CB, Middleton MS. In vivo characterization of the liver fat (1)H MR spectrum. NMR Biomed. 2011; 24:784–790. [PubMed: 21834002]
21. Yu, HS,A.; Hernando, D.; Hines, CDG.; McKenzie, CA.; Reeder, SB.; Brittain, JH. Noise Performance of Magnitude-based Water-Fat Separation is Sensitive to the Echo Times. Montreal, Canada: 2011. p. 2715
22. Hernando D, Hines CD, Yu H, Reeder SB. Addressing phase errors in fat-water imaging using a mixed magnitude/complex fitting method. Magn Reson Med. 2012; 67:638–644. [PubMed: 21713978]
23. Reeder SB, Sirlin CB. Quantification of liver fat with magnetic resonance imaging. Magn Reson Imaging Clin N Am. 2010; 18:337–357, ix. [PubMed: 21094444]
24. Reeder SB, Hu HH, Sirlin CB. Proton density fat-fraction: a standardized MR-based biomarker of tissue fat concentration. J Magn Reson Imaging. 2012; 36:1011–1014. [PubMed: 22777847]
25. Kuhn JP, Hernando D, Munoz Del Rio A, Evert M, Kannengiesser S, Volzke H, Mensel B, Puls R, Hosten N, Reeder SB. Effect of Multipeak Spectral Modeling of Fat for Liver Iron and Fat Quantification: Correlation of Biopsy with MR Imaging Results. Radiology. 2012; 265:133–142. [PubMed: 22923718]
26. Hernando D, Kramer HJ, Reeder SB. Multipeak Fat-Corrected Complex R2* Relaxometry: Theory, Optimization, and Clinical Validation. Magn Reson Med. 2013; 70:1319–1331. [PubMed: 23359327]
27. Hernando D, Kuhn JP, Mensel B, Volzke H, Puls R, Hosten N, Reeder SB. R2* estimation using “in-phase” echoes in the presence of fat: The effects of complex spectrum of fat. J Magn Reson Imaging. 2013; 37:717–726. [PubMed: 23055408]
28. Hines CD, Yu H, Shimakawa A, McKenzie CA, Brittain JH, Reeder SB. T1 independent, T2* corrected MRI with accurate spectral modeling for quantification of fat: validation in a fat-water-SPIO phantom. J Magn Reson Imaging. 2009; 30:1215–1222. [PubMed: 19856457]
29. Bernard CP, Liney GP, Manton DJ, Turnbull LW, Langton CM. Comparison of fat quantification methods: a phantom study at 3.0T. J Magn Reson Imaging. 2008; 27:192–197. [PubMed: 18064714]
30. Huppertz A, Haraida S, Kraus A, Zech CJ, Scheidler J, Breuer J, Helmberger TK, Reiser MF. Enhancement of focal liver lesions at gadoxetic acid-enhanced MR imaging: correlation with histopathologic findings and spiral CT--initial observations. Radiology. 2005; 234:468–478. [PubMed: 15591431]
31. Reimer P, Vosshenrich R. Detection and characterization of liver lesions using gadoxetic acid as a tissue-specific contrast agent. Biologics. 2010; 4:199–212. [PubMed: 20714357]
32. Raman SS, Leary C, Bluemke DA, Amendola M, Sahani D, McTavish JD, Brody J, Outwater E, Mitchell D, Sheafor DH, Fidler J, Francis IR, Semelka RC, Shamsi K, Gschwend S, Feldman DR, Breuer J. Improved characterization of focal liver lesions with liver-specific gadoxetic acid disodium-enhanced magnetic resonance imaging: a multicenter phase 3 clinical trial. J Comput Assist Tomogr. 2010; 34:163–172. [PubMed: 20351497]

33. Suh YJ, Kim MJ, Choi JY, Park YN, Park MS, Kim KW. Differentiation of hepatic hyperintense lesions seen on gadoxetic acid-enhanced hepatobiliary phase MRI. AJR Am J Roentgenol. 2011; 197:W44–52. [PubMed: 21700994]
34. Frydrychowicz A, Lubner MG, Brown JJ, Merkle EM, Nagle SK, Rofsky NM, Reeder SB. Hepatobiliary MR imaging with gadolinium-based contrast agents. J Magn Reson Imaging. 2012; 35:492–511. [PubMed: 22334493]
35. Hwang J, Kim SH, Lee MW, Lee JY. Small (</= 2 cm) hepatocellular carcinoma in patients with chronic liver disease: comparison of gadoxetic acid-enhanced 3.0 T MRI and multiphasic 64-multirow detector CT. Br J Radiol. 2012; 85:e314–322. [PubMed: 22167508]
36. Bluemke DA, Sahani D, Amendola M, Balzer T, Breuer J, Brown JJ, Casalino DD, Davis PL, Francis IR, Krinsky G, Lee FT Jr. Lu D, Paulson EK, Schwartz LH, Siegelman ES, Small WC, Weber TM, Welber A, Shamsi K. Efficacy and safety of MR imaging with liver-specific contrast agent: U.S. multicenter phase III study. Radiology. 2005; 237:89–98. [PubMed: 16126918]
37. Bashir MR, Husarik DB, Ziemlewicz TJ, Gupta RT, Boll DT, Merkle EM. Liver MRI in the hepatocyte phase with gadolinium-EOB-DTPA: does increasing the flip angle improve conspicuity and detection rate of hypointense lesions? J Magn Reson Imaging. 2012; 35:611–616. [PubMed: 22034383]
38. Frydrychowicz A, Jedynak AR, Kelcz F, Nagle SK, Reeder SB. Gadoxetic acid-enhanced T1-weighted MR cholangiography in primary sclerosing cholangitis. J Magn Reson Imaging. 2012; 36:632–640. [PubMed: 22581411]
39. Lee MS, Lee JY, Kim SH, Park HS, Kim SH, Lee JM, Han JK, Choi BI. Gadoxetic acid disodium-enhanced magnetic resonance imaging for biliary and vascular evaluations in preoperative living liver donors: comparison with gadobenate dimeglumine-enhanced MRI. J Magn Reson Imaging. 2011; 33:149–159. [PubMed: 21182133]
40. Idilman IS, Aniktar H, Idilman R, Kabacam G, Savas B, Elhan A, Celik A, Bahar K, Karcaaltincaba M. Hepatic steatosis: quantification by proton density fat fraction with MR imaging versus liver biopsy. Radiology. 2013; 267:767–775. [PubMed: 23382293]
41. Wells, SA.; Diego Hernando, D.; Vigen, KK.; Reeder, SB. Effect of Hepatocyte-Specific Gadolinium-Based Contrast Agents on Hepatic Fat-Fraction and R2*.. Proceedings of the 20th Annual Meeting of ISMRM; Melbourne, Australia. 2012; p. 4034
42. Burke, LMB.; Zhong, X.; Fananapazir, G.; Dale, BM.; Nickel, D.; Kannengiesser, SAR.; Bashir, MR. Robustness of a Hybrid Magnitude/complex Method for Liver Fat Quantification in the Presence of a Hepatobiliary Contrast Agent.. Proceedings of the 21th Annual Meeting of ISMRM; Salt Lake City, Utah. 2013; p. 4088
43. Malinchoc M, Kamath PS, Gordon FD, Peine CJ, Rank J, ter Borg PC. A model to predict poor survival in patients undergoing transjugular intrahepatic portosystemic shunts. Hepatology. 2000; 31:864–871. [PubMed: 10733541]
44. Brau AC, Beatty PJ, Skare S, Bammer R. Comparison of reconstruction accuracy and efficiency among autocalibrating data-driven parallel imaging methods. Magn Reson Med. 2008; 59:382–395. [PubMed: 18228603]
45. Holm S. A Simple Sequentially Rejective Multiple Test Procedure. Scandinavian Journal of Statistics. 1979; 6:65–70.
46. de Bazelaire CM, Duhamel GD, Rofsky NM, Alsop DC. MR imaging relaxation times of abdominal and pelvic tissues measured in vivo at 3.0 T: preliminary results. Radiology. 2004; 230:652–659. [PubMed: 14990831]
47. Wood JC, Enriquez C, Ghugre N, Tyzka JM, Carson S, Nelson MD, Coates TD. MRI R2 and R2* mapping accurately estimates hepatic iron concentration in transfusion-dependent thalassemia and sickle cell disease patients. Blood. 2005; 106:1460–1465. [PubMed: 15860670]
48. Weinmann HJ, Brasch RC, Press WR, Wesbey GE. Characteristics of gadolinium-DTPA complex: a potential NMR contrast agent. AJR Am J Roentgenol. 1984; 142:619–624. [PubMed: 6607655]
49. Hamilton, G.; Middleton, M.; Cunha, G.; Sirlin, C. Effect of gadolinium-based contrast agent on the relaxation properties of water and fat in human liver as measured in vivo by 1H MRS.. Proceedings of the 21st Annual Meeting of ISMRM; Salt Lake City, UT. 2013; p. 1516

50. Brismar TB, Dahlstrom N, Edsborg N, Persson A, Smedby O, Albiin N. Liver vessel enhancement by Gd-BOPTA and Gd-EOB-DTPA: a comparison in healthy volunteers. Acta Radiol. 2009; 50:709–715. [PubMed: 19701821]

51. Motosugi U, Ichikawa T, Sano K, Sou H, Onohara K, Muhi A, Kitamura T, Amemiya F, Enomoto N, Matsuda M, Asakawa M, Fujii H, Araki T. Double-dose gadoxetic Acid-enhanced magnetic resonance imaging in patients with chronic liver disease. Invest Radiol. 2011; 46:141–145. [PubMed: 21139506]

52. Frydrychowicz A, Nagle SK, D'Souza SL, Vigen KK, Reeder SB. Optimized high-resolution contrast-enhanced hepatobiliary imaging at 3 tesla: a cross-over comparison of gadobenate dimeglumine and gadoxetic acid. J Magn Reson Imaging. 2011; 34:585–594. [PubMed: 21751288]

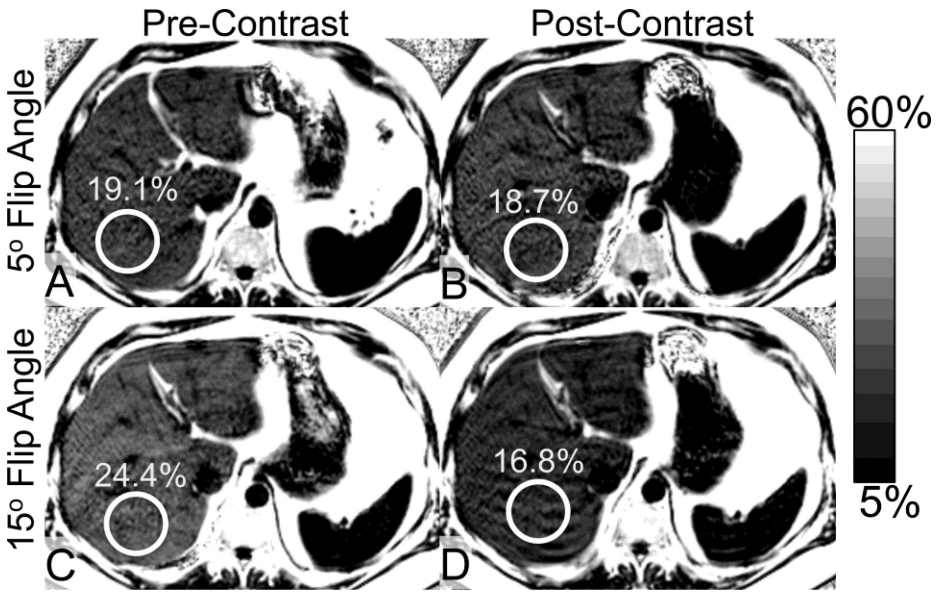

Figure 1.

Representative example of fat-fraction maps acquired at 5° flip and 15° flip angles, before and after intravenous administration of gadoxetic acid in a 43-year-old man with hepatic steatosis (PDFF of 19.1%, based on pre-contrast low flip angle acquisition). (a,b) There is no significant change in PDFF after contrast, when low flip angles are used. However, the apparent FF increases at high flip angles (c) prior to contrast, and, (d) decreases paradoxically following the administration of contrast when high flip angles are used.

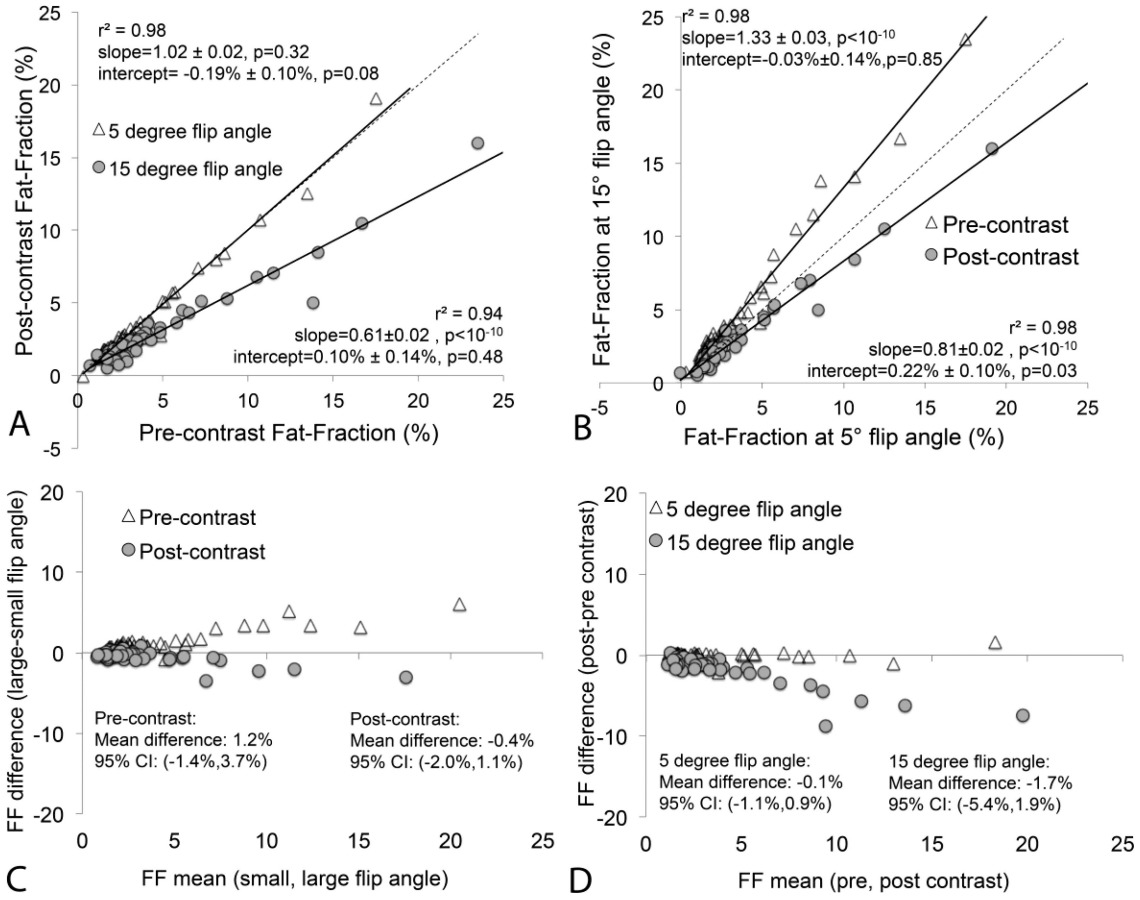

Figure 2.

Scatterplots demonstrate hepatic fat-fractions obtained at low (5°) and high (15°) flip angles before and after the administration of gadoxetic acid. (a) Hepatic fat-fraction is not affected by contrast when T1 related bias is avoided at low flip angles. (b) At high flip angles, hepatic fat-fraction is overestimated prior to contrast and underestimated after contrast administration. This implies that, in the presence of gadoxetic acid in the liver, the T1 of water becomes shorter than the T1 of fat. The dashed line is the line of unity. (c) Bland-Altman analysis comparing low flip angle to high flip angle FF estimates, both before and after contrast. (d) Bland-Altman analysis comparing FF estimates before and after contrast, both using low and high flip angle acquisitions. Note the excellent agreement of T1-independent (ie: low flip angle) fat quantification performed before and after contrast administration.

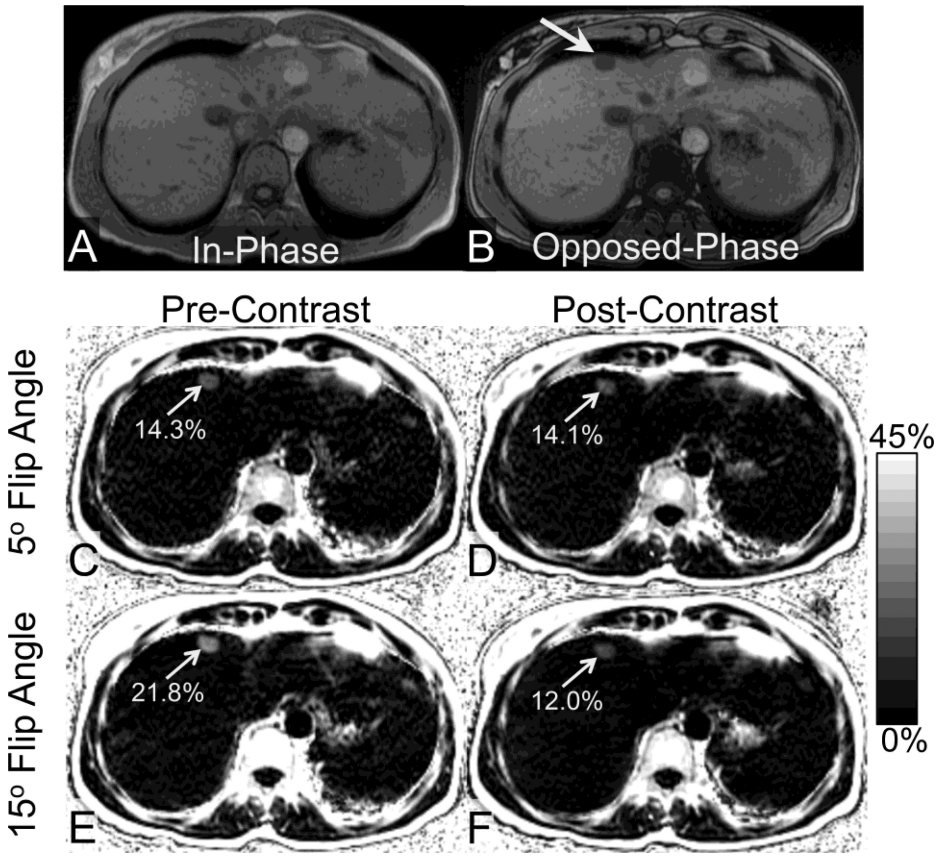

Figure 3.

An area of focal fat in segment IVa of the liver (arrow) is seen on in- and opposed phase imaging (a,b) in the liver of a 44 year old woman. The PDFF of the focal fat measured from the pre-contrast low flip angle FF map is 14.3%. No significant change is seen after contrast when a low flip angle is used (c,d). However, when a high flip angle is used, the FF is overestimated prior to contrast (e), and underestimated when acquired in the delayed hepatobiliary phase after administration of gadoxetic acid (f).

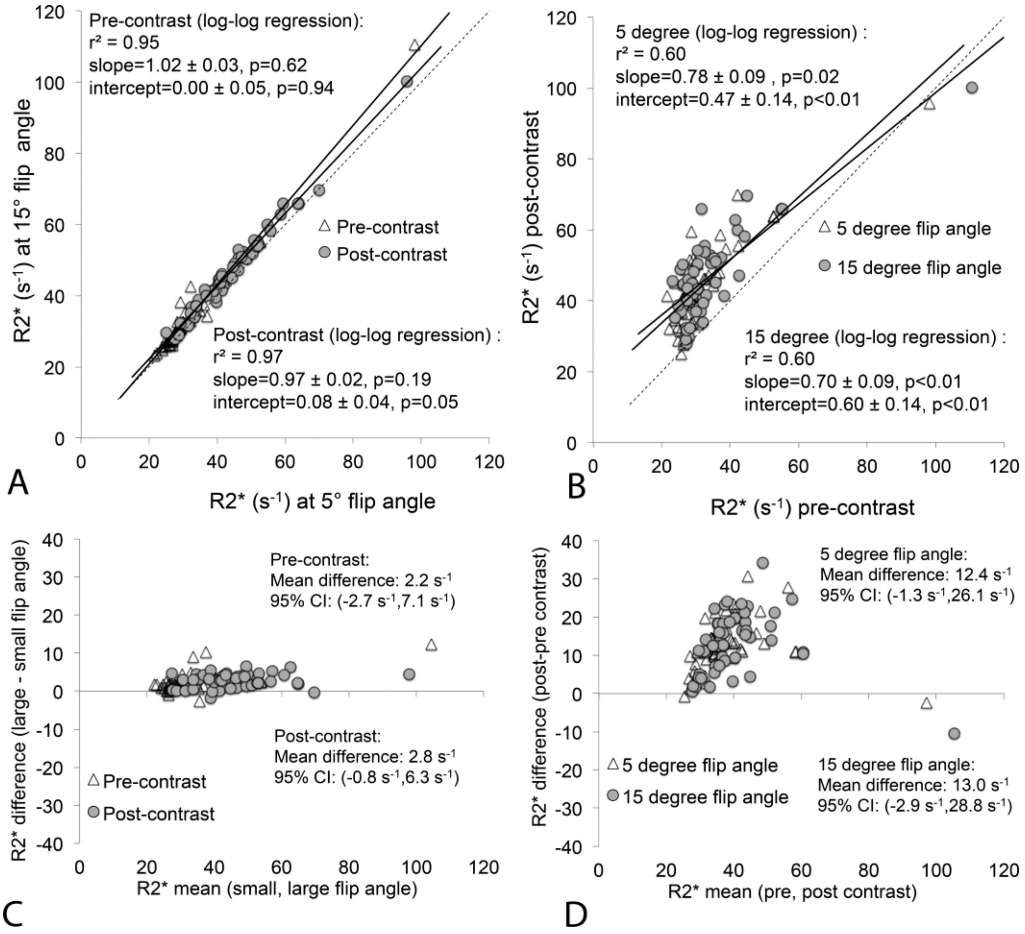

Figure 4.

Comparison between hepatic R2* obtained at low (5°) and high (15°) flip angles before and after the administration of gadoxetic acid. There is no substantial difference in hepatic R2* at low and high flip angles; however, there is significant increase in hepatic R2* following contrast administration at both flip angles. (a) Scatterplot of R2* acquired with low vs high flip angle (both pre- and post-contrast). (b) Scatterplot of R2* pre-contrast vs post-contrast (for low and high flip angles). Dashed line equals the line of unity. (c) Bland-Altman analysis comparing low flip angle to high flip angle R2* estimates, both before and after contrast. (d) Bland-Altman analysis comparing R2* estimates before and after contrast, both using low and high flip angle acquisitions.

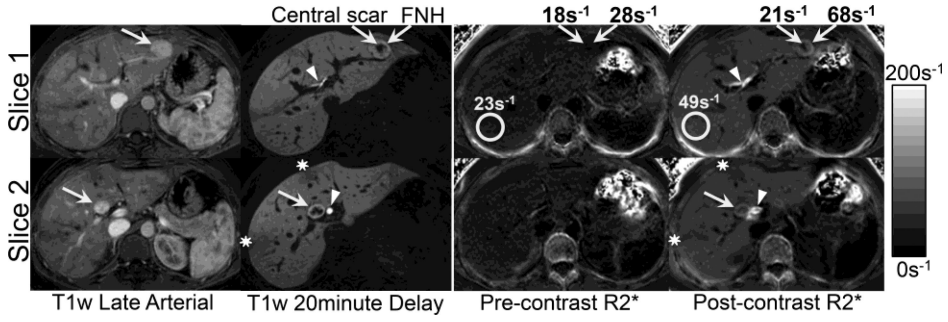

Figure 5.

Dynamic postcontrast enhanced (late arterial and 20 minute delayed phases) T1-weighted MR images acquired in a 26 year old female demonstrate uniform early enhancement with progressive accumulation of gadoxetic acid in two hepatic masses (segment III and IVb) with a central scar, diagnostic for focal nodular hyperplasia. R2* maps acquired before and after gadoxetic acid show an increase in the R2* in the background liver from $23s^{-1}$ to $49s^{-1}$, and also an increase in R2* of the lesions from $28s^{-1}$ to $68s^{-1}$, with little increase in the central scar. This indicates slightly higher uptake/retention of gadoxetic acid in the lesions compared to background liver, consistent with the qualitative behavior of T1 weighted imaging.

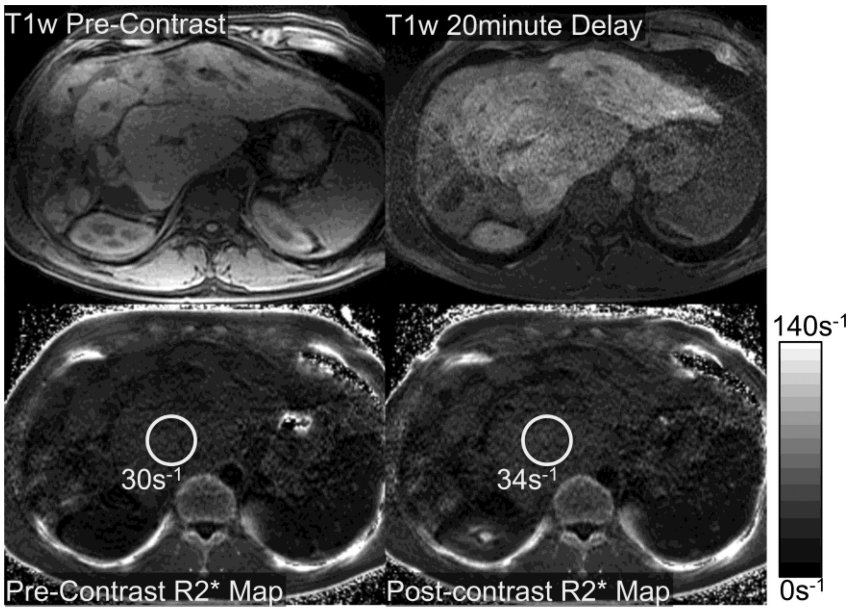

Figure 6.

Relatively poor uptake of gadoxetic acid was observed in a 36 year old man with primary sclerosing cholangitis and hepatic dysfunction: total bilirubin=2.5 mg/dL, ALT = 76 U/L, AST = 97 U/L, alkaline phosphatase = 384 U/L, INR=1.1, albumin = 2.6 g/dL, platelets=209× 10^9 /L, and a calculated MELD score of 11. As seen on the T1 weighted images and the R2* maps, the uptake of gadoxetic acid was very heterogeneous and very low, increasing from only $30s^{-1}$ to approximately $34s^{-1}$.

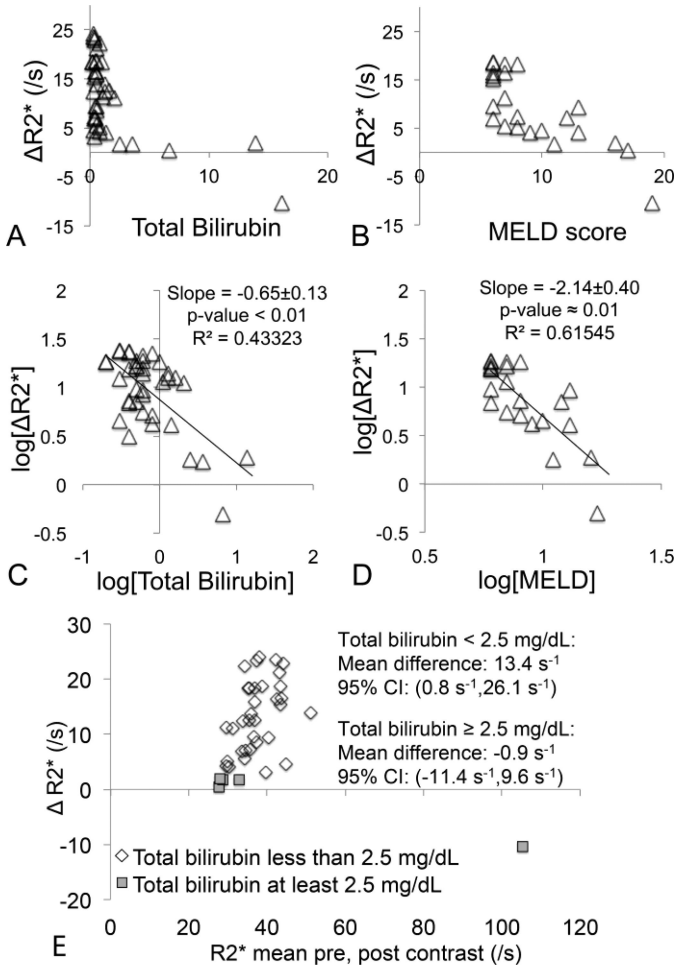

Figure 7.

Comparison between imaging and blood analysis measurements, including scatterplots of (a) ΔR2* vs total bilirubin, and (b) ΔR2* vs MELD score. Also shown are logarithm-domain linear regressions for the same comparisons (excluding the one value ΔR2*<0): (c) ΔR2* vs total bilirubin, and (d) ΔR2* vs MELD score. Finally, (e) shows Bland-Altman analysis for ΔR2* performed separately for groups of patients with total bilirubin <2.5 mg/dL (33 patients) and ≥2.5 mg/dL (5 patients), respectively. In the first group there is a significant increase in R2* post-contrast, whereas in the second group there is no increase in R2*. Only high flip angle R2* was analyzed here for brevity.

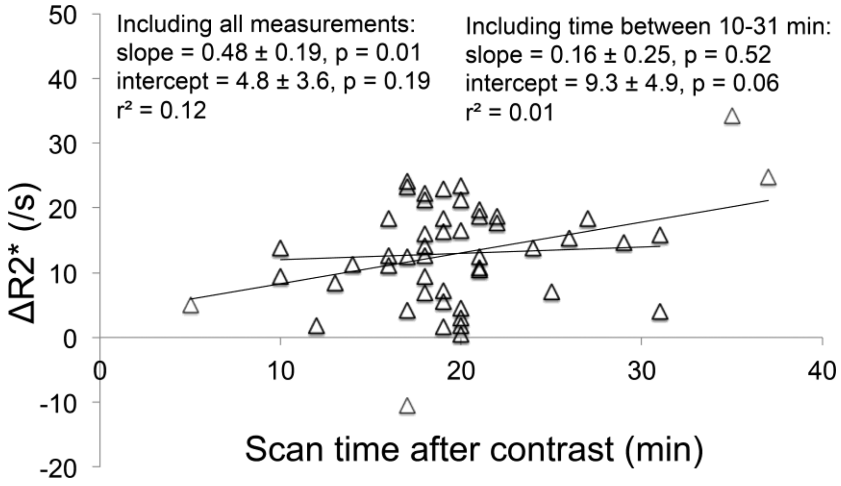

Figure 8.

Comparison between the delay time after contrast (in minutes) and ΔR2* (in s^{-1}). Including very short (<10 min) and very long (>34 min) times results in a significant increase in ΔR2* with time after contrast (p=0.01), but excluding these extreme values results no significant correlation between ΔR2* and time after contrast (p=0.52).